NUMERICAL INVESTIGATION OF VIBRATIONAL MODES AND SOUND RADIATION IN A GAMELAN GONG

[a)]Laurentius Kevin Hendinata

[a)]Centrale Méditerranée, Aix Marseille Université, 13013 Marseille, France,
laurentius-kevin.hendinata@etu.univ-amu.fr

ABSTRACT

The gamelan gong holds a central place in Javanese musical and cultural traditions, serving both as a sonic landmark and a symbol within ritual performances. This study numerically investigates the gong's vibrational behavior and acoustic radiation using a finite element model that captures the coupled structural-acoustic dynamics under realistic boundary conditions. Structural dynamics and coupled acoustic simulations uncover a fundamental mode at 233 Hz, where motion concentrates in the central boss and yields a deep, slowly decaying tone that underpins the ensemble's cycle. Two higher resonances at 1546 Hz and 2738 Hz exhibit increasingly intricate nodal patterns, producing sharply peaked sound pressure levels up to 150 dB and generating the inharmonic partials that give the gong its characteristic shimmer. Quantitative comparison with ethnomusicological measurements confirms frequency ratios of approximately 6.6 and 11.8 relative to the fundamental.

KEYWORDS

Gong, Javanese gamelan, vibrational modes, acoustic radiation

1. INTRODUCTION

Gamelan is a traditional musical ensemble from Indonesia, known for its unique sound and layered rhythmic structure. It consists mainly of tuned percussion instruments made from bronze or iron [1], [2], [3]. It exists in several regional forms, including Javanese, Balinese, Sundanese, and others, each with unique styles, tunings, and cultural meanings. The ensemble is not only a musical system but a symbolic expression of communal and spiritual values.

Within the gamelan ensemble, a variety of percussion instruments coexist. A standard gamelan ensemble typically includes metallophones, xylophones, kendang (drums), saron, bonang, gender, rebab (bowed string instrument), suling (bamboo flute), and gongs [3], [4]. These physical differences lead to a distinctive range of fundamental frequencies and overtone structures, creating a rich sonic palette.

Among its instruments, the gong occupies a central role, both sonically and symbolically. In Javanese gamelan, large gongs with a central raised boss (called *penclon*) serve as temporal anchors. Their function is not melodic but structural: they mark the culmination of musical cycles, known as gongan, and signal key moments in performance [5]. The striking of a gong signifies a transition, often aligning with ritual time or the turning of a narrative phrase. The instrument is deeply embedded in cultural practice and is often associated with ideas of cosmic balance, ancestral presence, and sacred space [6], [7], [8]. Its resonant, slowly decaying tone is considered essential for grounding the ensemble and connecting the physical and spiritual realms during performance.

From a physical perspective, the gong presents a compelling object of study. It combines a curved shell geometry with nonuniform thickness, leading to a rich and complex vibrational response. When struck, it supports a range of vibrational modes, some of which couple efficiently with the surrounding air to produce strong acoustic radiation. The vibrational energy is initially concentrated in the central boss, then propagates across the body of the gong [9], [10], [11]. The resulting acoustic field reflects both the structural dynamics of the plate and its interaction with air as a radiating surface [12].

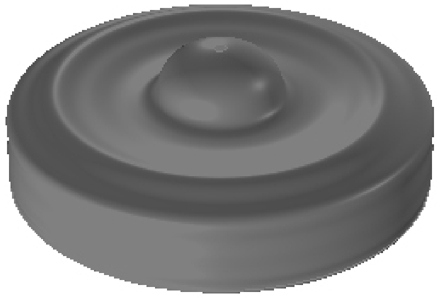

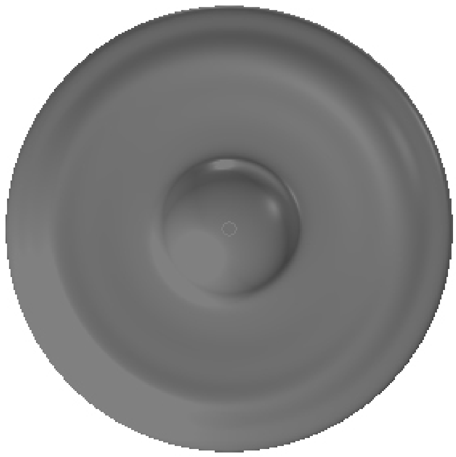

This study applies FEM to analyze the vibroacoustic response of a traditional Javanese gong. It identifies natural frequencies and mode shapes under support conditions resembling physical suspension. The study also simulates forced vibration at the gong's central boss and evaluates the resulting acoustic pressure field. Through this approach, the work aims to connect structural vibration patterns with audible features such as pitch salience and overtone richness.

2. GEOMETRIC AND MATERIAL CONFIGURATION

2.1. GEOMETRY DEFINITION

The gong analyzed in this study is a moderately sized example from the Javanese gamelan family, selected to represent typical structural features while maintaining computational efficiency. The model geometry is based on a direct measurement of a physical instrument. The overall radius of the gong is set at 10.5 cm, with a central boss (or penclon) radius of 2.2 cm. The gong's thickness is not uniform, varying from approximately 0.20 cm at the rim to 0.30 cm at the boss, following a gradual contour that is typical of handcrafted gongs.

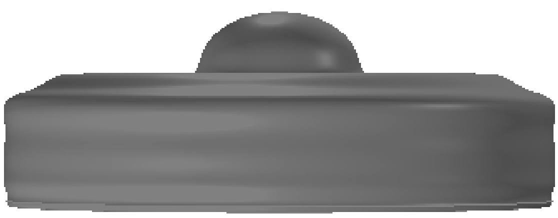

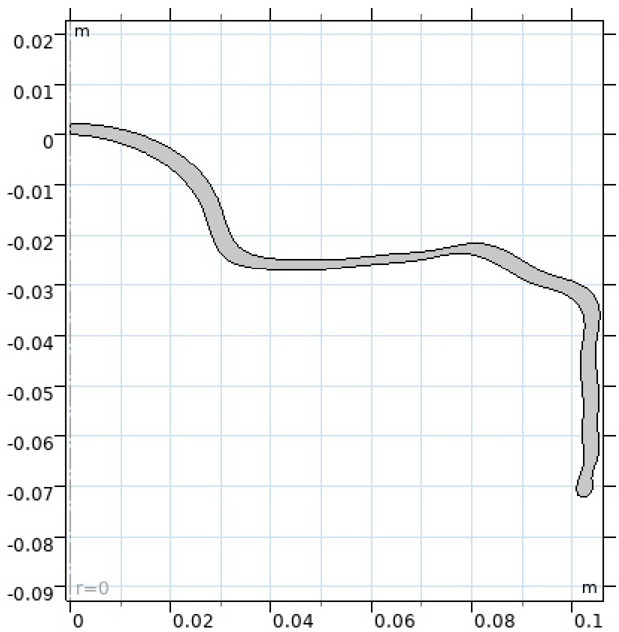

Fig. 1: Illustration of the traditional gamelan gong (a) orthogonal views and the top-side plane perspectives, and (b) cross-sectional profile modeled in 2D axisymmetric coordinates.

The geometry is represented using a 2D axisymmetric model (Figure 1b), which captures the essential profile of the gong while assuming perfect rotational symmetry. This approach simplifies computation and is appropriate for capturing the dominant radial and circumferential modes in an idealized structure. However, it does not account for three-dimensional irregularities such as local warping, material anisotropy, or slight asymmetries introduced during traditional casting and manual tuning.

2.2. MATERIAL PROPERTIES

Traditional Javanese gongs are cast from a high-tin bronze alloy, typically comprising 78% copper and 22% tin by weight. This alloy selection balances high stiffness and acoustic brightness with the castability required for detailed shaping. Tin increases the alloy's hardness and elevates its elastic modulus, while copper ensures sufficient density and ductility. In some cases, trace elements such as zinc or lead are included in small amounts to improve fluidity during casting or influence internal damping. The specific alloy composition used in gamelan manufacturing has been refined over generations to optimize both mechanical stability and tonal richness.

This specific alloy composition forms the basis for our simulation parameters. The density of 8800 kg/m³ reflects the heavy copper content. Young's modulus of 110 GPa captures the combined stiffness of copper and tin in the alloy. Poisson's ratio of 0.34 characterizes its lateral contraction under load. These values are consistent with published data for high-tin bronzes used in musical applications. The material is assumed to be isotropic and homogeneous, a simplification that ignores potential grain orientation or segregation effects, which may arise during solidification or manual finishing.

To represent internal energy loss, an isotropic structural loss factor of 0.04 is applied. This damping term accounts for internal friction, arising primarily from dislocation motion, grain boundary sliding, and minor inelastic effects within the metallic microstructure. It does not include radiation damping, which is treated separately in the acoustic simulation.

3. MODAL ANALYSIS

3.1. MARKING OF IMAGES

The finite element model is developed using a 2D axisymmetric approach to capture the gong's cross-sectional geometry. The solid domain is assigned bronze material properties based on the alloy specifications described earlier. An eigenfrequency solver based on the Arpack method is used to extract the natural frequencies and associated mode shapes.

The boundary condition applied is a simply supported outer edge, implemented by constraining radial displacement at the rim (u_r = 0), while allowing vertical motion and rotation. This setup approximates the real-world suspension of a gong by cords at discrete points around its edge, which imposes minimal constraint on its vertical motion but provides support in the plane of the plate. The central boss remains entirely free, mimicking how the striking zone moves during performance.

The mesh is constructed using a swept triangular element scheme, with quadratic Lagrange elements to improve accuracy in capturing curvature and localized bending. The mesh is refined significantly near the boss and shoulder transitions, where mode localization and curvature effects dominate. A mesh convergence study was conducted by systematically refining the element size and observing the change in the first few natural frequencies. Convergence was achieved with less than 0.5% deviation in frequency values upon further refinement, confirming mesh-independence of the results.

No pre-stress or residual stress conditions were included in this initial analysis. While residual stresses from casting and tuning could influence real-world frequencies slightly, they are neglected here to focus on geometry-driven modal behavior.

3.2. RESULTS

The finite element model is developed using a 2D axisymmetric approach to capture the gong's cross-sectional geometry. The solid domain is assigned bronze material properties based on the alloy specifications described

The computed mode shapes reveal distinct nodal circles and diameters that correspond to the gong's harmonic spectrum. The fundamental mode concentrates displacement in the central boss, matching the deep bass resonance valued in Javanese ceremonies. Higher modes form complex patterns that distribute vibrational energy across the plate, enriching overtone content.

The simulated natural frequencies and mode shapes of the gong show clear vibrational patterns consistent with the behavior of circular plates that have non-uniform thickness. Table 1 presents the first three modes from the results. The lowest frequency is 233.04 Hz, followed by 1545.60 Hz and 2737.80 Hz. This wide frequency range reflects the contrast in stiffness between the central boss and the rest of the plate.

The first mode at 233.04 Hz shows strong displacement localized at the central boss, with minimal movement in the outer regions. This is a typical piston-like mode, where the boss moves in and out while the surrounding plate acts as a relatively rigid support. Physically, the boss behaves as a mass-loaded center, reducing the system's effective stiffness in the region and lowering the frequency. The outer plate's thickness and radial stiffness suppress significant motion, resulting in a deep, sustained tone with relatively low radiation efficiency.

The second mode, near 1545.60 Hz, features a large vibrating region across much of the plate surface, including the dome and shoulder areas. Several nodal diameters and one or two nodal circles can be identified. This pattern allows more efficient coupling with the surrounding air, and as such, this mode corresponds to the most acoustically prominent pitch of the gong. It produces the sharp, striking tone often used to mark phrase boundaries in Javanese musical cycles.

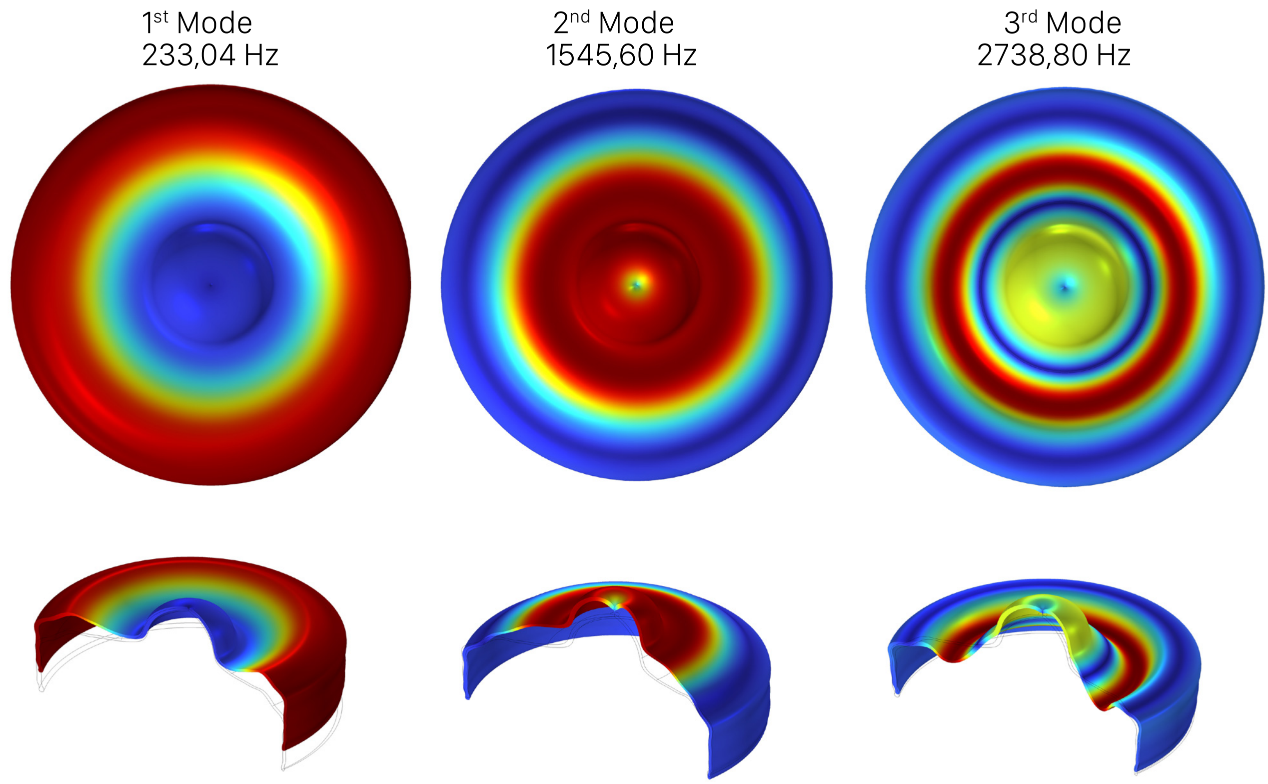

Fig. 2: First three modes of the gamelan gong.

At 2737.80 Hz, the third mode exhibits a more fragmented pattern, with multiple nodal circles and diameters. The vibrational energy is distributed in smaller lobes across the plate, contributing to inharmonic overtones and the rich metallic timbre of the gong.

The frequency ratios of the modes deviate significantly from those expected for an ideal circular plate with uniform thickness. In theory, for a thin isotropic plate with clamped or simply supported boundaries, the second and third frequencies would occur at approximately 2.0 and 3.5 times the first mode, depending on boundary conditions and aspect ratio. However, in this case, the second mode occurs at 6.6 times the first, and the third at 11.7 times, indicating strong modal inharmonicity.

The inharmonicity observed in the modal frequencies arises from a combination of geometric and material factors. First, the plate's non-uniform thickness introduces variations in local bending stiffness, which causes certain higher-order modes to shift upward more significantly than others. In contrast, the central boss acts as a concentrated mass, lowering the fundamental frequency more than it affects the higher modes, thus widening the gap between them. Additionally, the combined influence of internal damping and the complex curvature of the gong disrupts the regular spacing of natural frequencies typically found in idealized circular plates, further reinforcing the inharmonic structure that characterizes the gong's acoustic signature.

Such inharmonic spacing is intentional and musically significant in gamelan instruments. The perceived intervals and pitch centers differ from Western scales, and the modal structure here supports that cultural usage. In practice, the asymmetry and minor imperfections in the real instrument further split these modes, leading to beating phenomena and spectral richness that are prized in performance.

4. FORCED VIBRATION AND TRANSFER FUNCTION ANALYSIS

4.1. EXCITATION SETUP

To study the gong's response under external loading, a forced vibration analysis was carried out using a harmonic excitation approach. The excitation was applied as a point force directly at the center of the dome, which is the usual striking point during a performance. Although percussive impacts happen in the time domain, a harmonic sweep in the frequency domain was chosen because it allows detailed observation of the system's steady-state response at each frequency. This method is useful for identifying resonances, and its results can later be related to time-domain behavior through Fourier analysis.

The excitation force was set with a fixed amplitude and zero phase shift. Because the model assumes linear behavior, the response scales proportionally with the force, and only the relative amplitude and phase are important. A sweep from 50 Hz to 2000 Hz was used to cover both the fundamental mode and several higher modes that contribute to the gong's sound. This range was chosen to capture the bass and overtone content typically heard in performance and to stay within the lower part of the human hearing range, where most of the gong's energy lies.

Displacement results were monitored at three locations: the dome rim, the shoulder (where the dome transitions to the flat plate), and the outer edge of the gong. These points were selected to track how vibrations spread from the impact point across the surface. They also provide useful data for evaluating transfer functions, which show how energy moves through the structure and where it tends to concentrate or fade out.

4.2. TRANSFER FUNCTION EVALUATION

The transfer function describes how much motion occurs at one point on the gong in response to a force applied at another. It is defined as the ratio between the displacement magnitude at a given location and the applied harmonic force. Mathematically, it takes the form as in Eq. (1).

$$H(f) = \frac{U_{resp}(f)}{F_{input}(f)} \quad (1)$$

where $U_{resp}(f)$ represents the frequency-dependent displacement amplitude at the observation point and $F_{input}(f)$ is the magnitude of the applied excitation force. This formulation allows quantification of how effectively vibrations propagate from the excitation site to other parts of the gong's structure.

By plotting both the magnitude and phase of the transfer function over the swept frequency range, resonant peaks corresponding to natural vibration modes can be identified. These peaks indicate frequencies at which the gong responds strongly to excitation, highlighting modal contributions to the overall vibro-acoustic behavior. The phase information provides insight into the relative timing of displacement responses, which is important for understanding wave propagation and mode coupling within the instrument.

more coherent motion across the plate, leading to stronger radiation and a clearer peak in the sound pressure spectrum.

The spacing between these peaks does not follow simple harmonic ratios, which is typical for plates and shells with curved and non-uniform geometry. In these systems, the modal frequencies are determined by complex relationships involving stiffness, mass distribution, and boundary conditions. As a result, the gong produces a rich set of inharmonic overtones that contribute to its unique timbre, different from the harmonic series found in string or air column instruments.

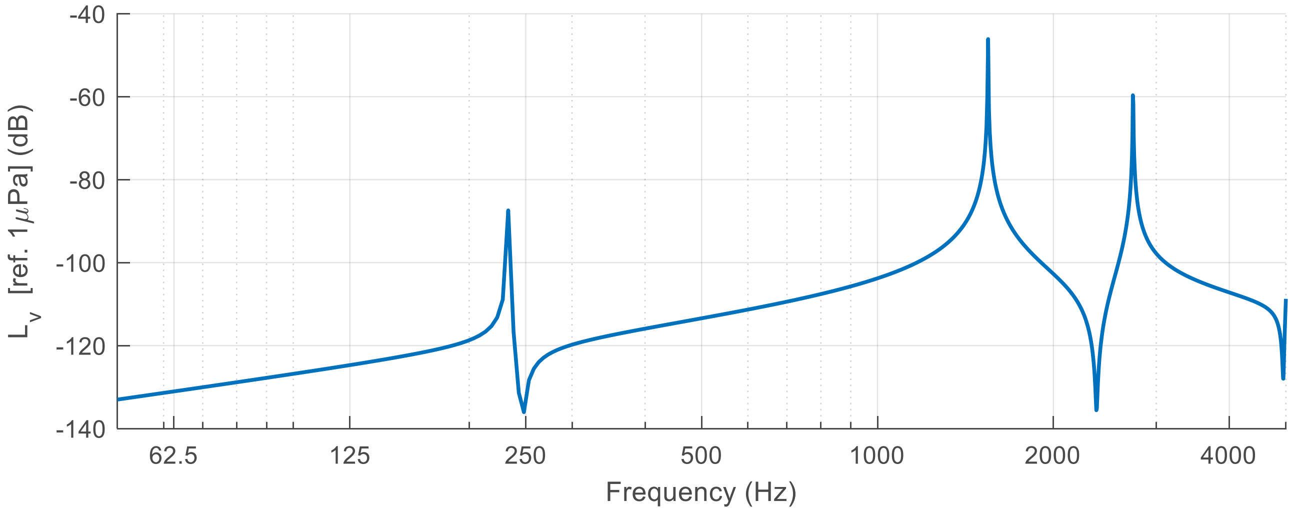

Fig. 3: Vibration level distribution on the gong arm.

Figure 3 shows the vibration levels recorded at the outer region of the gong. The first clear resonance appears around 250 Hz, but the amplitude is relatively low, about −85 dB. In contrast, the strongest response is found near 1700 to 1800 Hz, where the displacement level rises to about −45 dB. Other peaks appear around 2500 Hz and close to 4000 Hz, but with lower intensity, typically near −60 dB. These frequencies correspond to the system's natural modes and reflect how the structure responds to excitation, based on its shape and material properties.

The variation in peak amplitudes shows that not all modes radiate sound equally well. The low-frequency mode near 250 Hz causes mostly localized movement in the central dome. While this motion is strong within the plate, it often leads to weak sound radiation due to destructive interference. Opposite parts of the surface may move out of phase, cancelling each other's acoustic output. In contrast, the higher-frequency mode near 1700 Hz appears to couple better with the surrounding air. Its vibration pattern may involve

5. ACOUSTIC COUPLING AND SPL ESTIMATION

To simulate the conversion of mechanical vibration into radiated sound, a coupled structural-acoustic analysis is performed in the frequency domain. The solid domain represents the gong's bronze shell, governed by the Navier-Cauchy equations for linear elasticity. The surrounding air domain is modeled using the Helmholtz equation for time-harmonic pressure fields. The two domains are coupled through boundary conditions that ensure physical continuity at their interface. Specifically, the normal velocity of the vibrating shell must match the fluid particle velocity, and the stress in the solid must balance the pressure-induced traction in the fluid.

The air domain extends approximately 2 meters from the center of the gong in all directions. To simulate an unbounded acoustic space, radiation boundary conditions are applied at the outer boundaries. These are implemented using perfectly matched layers (PML) that absorb outgoing waves without reflection, mimicking open-air conditions. This treatment avoids artificial interference from wave reflections at the domain edge and improves the accuracy of radiated sound predictions.

The coupled problem is solved using the finite element method, where the solid and fluid domains are meshed and computed simultaneously. The FEM solver handles the direct coupling of degrees of freedom at the solid-fluid boundary, ensuring energy transfer across the interface is correctly modeled. This approach captures the mutual interaction between vibration and sound radiation.

To evaluate sound radiation quantitatively, pressure is monitored at several points placed on a circular probe line 1 meter above the gong apex. The selected distance approximates a typical listening position and ensures measurements are taken in the acoustic far field. Probe points are evenly distributed along the circumference to capture angular variations in pressure and avoid bias from directional radiation. The pressure magnitude at each frequency $p(r,f)$ is recorded and converted to sound pressure level (SPL) using the standard expression, as in Eq. (2).

$$SPL\ (f) = 20\log_{10}\left(\frac{|p(r,f)|}{p_{ref}}\right) \quad (2)$$

where $p_{ref} =$ 20μPa is the reference sound pressure. An average SPL over all probe points is taken to provide a representative measure of the radiated acoustic energy at each frequency.

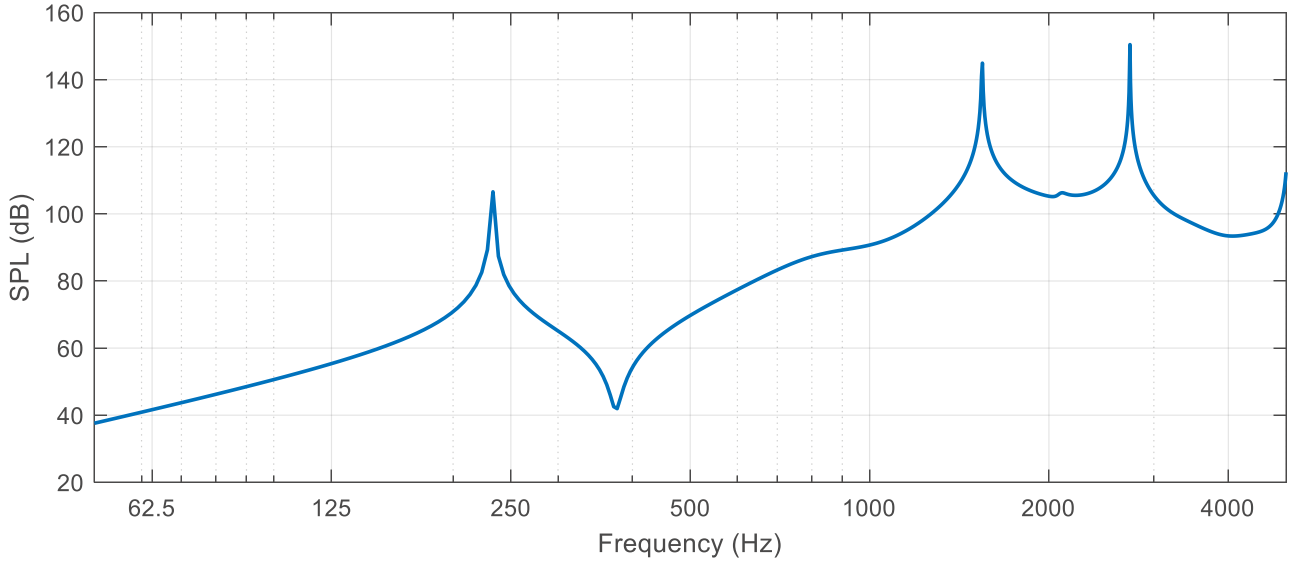

Fig. 4: SPL measured at 1 meter above the gong apex during shell excitation.

Figure 4 presents the SPL measured at 1 meter above the gong following harmonic excitation. The spectrum shows several peaks, each indicating a strong acoustic response. These peaks align with structural resonances where surface motion efficiently couples to the surrounding air. The most prominent peak appears between 1700 and 1800 Hz, corresponding to a vibration mode that radiates sound effectively due to its coherent surface motion.

The third peak, at 2737 Hz, arises from a more fragmented mode with several nodal lines. While less efficient than the second mode, it still contributes to the overall sound character. A fourth peak appears near 3500 to 4000 Hz and likely represents higher-order patterns that radiate due to their higher frequency and surface area involvement.

Between these peaks, distinct dips are visible in the SPL. At 377 Hz, 1997 Hz, and 4058 Hz,

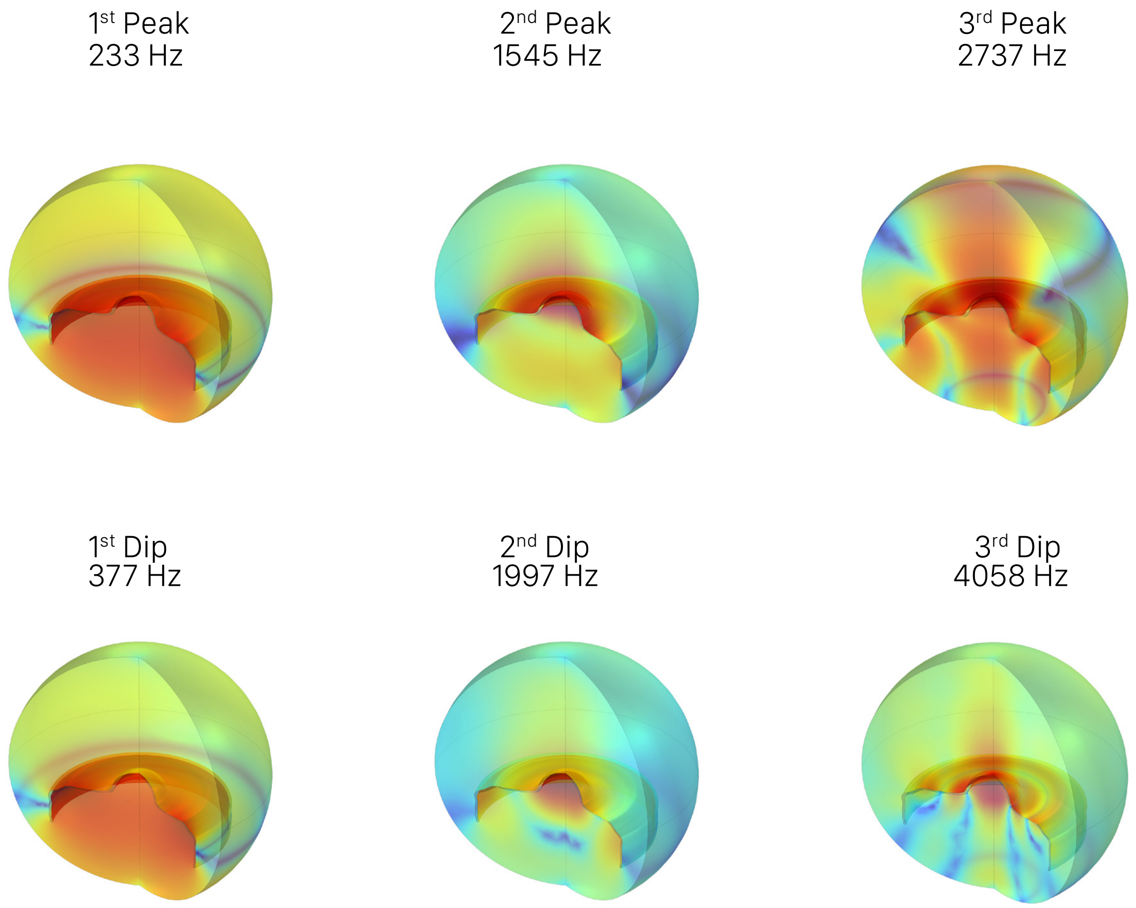

Fig. 5: Mode shapes of the gong shell at key resonance frequencies corresponding to peaks and dips in the SPL spectrum.

Figure 5 shows the mode shapes associated with key SPL features. For example, the first peak at 233 Hz corresponds to a low-order mode concentrated near the boss. Although structurally dominant, this mode produces limited sound because surface motion is mostly localized and generates minimal net air displacement. The second peak near 1546 Hz displays a broader pattern with most of the shell moving in phase. This mode behaves like a monopole source, pushing air uniformly and maximizing radiation efficiency.

the measured pressure drops sharply. These dips correspond to modes where adjacent regions on the gong surface move out of phase. This leads to destructive interference in the radiated field, a phenomenon similar to dipole or quadrupole cancellation. In such cases, the radiated sound waves cancel each other in certain directions, reducing net sound output despite significant vibration.

The correlation between mode shapes and SPL behavior highlights the role of radiation impedance. At peak frequencies, the gong's surface impedance matches well with the acoustic load, allowing efficient energy transfer. At dip frequencies, mismatched impedance and out-of-phase motion hinder radiation. These observations explain the uneven SPL response and the rich, inharmonic timbre of the gong.

Lastly, the slight discrepancy between the first vibration mode at 233 Hz and the first SPL peak near 250 Hz likely results from damping and coupling effects in the full system. While the modal analysis identifies the structural resonance, actual sound radiation depends on how effectively that mode excites pressure waves in air.

6. DISCUSSION

The gong's vibration behavior is shaped by its geometry, material distribution, and mass loading at the boss. The lowest mode, observed near 233 Hz, is mainly concentrated around the central boss. The added mass in this area reduces the natural frequency significantly. Most of the peripheral surface remains nearly stationary in this mode, which limits its ability to transfer energy into the air. As a result, this mode does not radiate sound efficiently. However, it plays an important perceptual role. It adds a tactile sensation when the gong is played and forms a deep spectral foundation that supports the higher components of the sound. While not clearly audible as a pitch, this mode adds depth and a sense of physical presence to the sound.

The mode at approximately 1546 Hz shows a much broader and more coherent motion across the shell. Its simple nodal pattern allows large surface regions to move in phase, making this mode highly efficient in radiating sound. This efficiency explains the prominent peak in the SPL spectrum. In performance, this mode produces the most clearly perceived pitch. It behaves as the "singing mode" of the gong and is often interpreted by listeners as the fundamental tone, even though it is not the lowest in frequency. This auditory dominance is due to its strong acoustic output and the human ear's sensitivity to frequencies in this range.

At higher frequencies, such as 2737 Hz and above, the mode shapes become increasingly complex. These higher modes contain multiple radial and circumferential nodal lines, breaking the shell into many segments that move in alternating directions. This fragmented motion causes the radiated pressure field to include a set of inharmonic overtones. These partials are not evenly spaced in frequency, unlike those from simple vibrating plates. Their irregular distribution contributes to the shimmering, evolving quality of the gong's sound. Though they carry less acoustic energy than the main mode at 1546 Hz, they are crucial for the instrument's timbre and richness.

These acoustic properties are closely linked to the cultural function of the gong. The prominent mode near 1546 Hz is tuned to match an interval in the Javanese slendro scale, rather than a note from Western tuning systems. In gamelan music, this pitch helps define musical structure. It marks time divisions within the gong and supports the ensemble's coordination. The deep 233 Hz component, while not clearly melodic, helps create a background sound that supports the ceremonial or meditative context of performance. Together, the inharmonic spectrum and sustained resonance of the gong support its role in both musical and spiritual dimensions.

From a design perspective, the gong's acoustic behavior reflects deliberate shaping of its physical structure. The thickness varies across the surface, and the boss adds asymmetry and mass, both of which shift the frequencies of key modes. These features seem intentionally designed to produce a complex, inharmonic spectrum suited to the instrument's function in gamelan music. The combination of structural and acoustical features supports ideas of balance, depth, and sonic presence, which are valued in the cultural context.

7. CONCLUSIONS

The finite element analysis identified the gamelan gong's natural frequencies and mode shapes. The fundamental mode near 233 Hz localizes vibration in the central boss, producing the culturally significant deep tone.

Higher modes at approximately 1546 Hz and 2738 Hz create inharmonic overtone patterns that enrich the sonic texture. The predicted sound pressure level spectrum matches well with known acoustic behavior, showing resonant peaks at these frequencies. These results quantitatively explain the gong's inharmonicity and modal distribution, confirming that its geometry and material properties critically shape its vibrational and acoustic response.

REFERENCES

1. R. A. Sutton, "Gamelan: The Traditional Sounds of Indonesia (review)," *Asian Music,* vol. 38, no. 1, pp. 142–144, 2007, Accessed: Jul. 25, 2025. [Online]. Available: https://muse.jhu.edu/pub/15/article/216426

2. H. Spiller and E. A. Clendinning, *Focus: Gamelan Music of Indonesia*, 3rd ed. New York: Routledge, 2022. doi: 10.4324/9781003014836.

3. D. W. Krueger, K. L. Gee, and J. Grimshaw, "Acoustical and vibrometry analysis of a large Balinese gamelan gong," *J. Acoust. Soc. Am.*, vol. 128, no. 1, pp. EL8–EL13, Jun. 2010, doi: 10.1121/1.3425742.

4. Sumarsam, "Inner Melody in Javanese Gamelan Music," *Asian Music,* vol. 7, no. 1, pp. 3–13, 1975, doi: 10.2307/833922.

5. J. Becker and A. Becker, "14. A Musical Icon: Power and Meaning in Javanese Gamelan Music," in *The Sign in Music and Literature*, W. Steiner, Ed., University of Texas Press, 2014, pp. 203–215. Accessed: Jul. 25, 2025. [Online]. Available: https://www.degruyterbrill.com/document/doi/10.7560/775633-014/html

6. D. Simons, *Gong Culture: A Survey of East Asian Gong Traditions*. 2009.

7. S. P. Walton, "Aesthetic and Spiritual Correlations in Javanese Gamelan Music," *J. Aesthet. Art Crit.*, vol. 65, no. 1, pp. 31–41, Sep. 2007, doi: 10.1111/j.1540-594X.2007.00235.x.

8. J. Becker, "Earth, Fire, Śakti, and the Javanese Gamelan," *Ethnomusicology,* vol. 32, no. 3, pp. 385–391, 1988, doi: 10.2307/851938.

9. D. W. Krueger, K. L. Gee, and J. Grimshaw, "Acoustical and vibrometry analysis of a large Balinese gamelan gong," *J. Acoust. Soc. Am.*, vol. 128, no. 1, pp. EL8–EL13, Jun. 2010, doi: 10.1121/1.3425742.

10. G. Tsai, B. Wang, Y. Lee, and Z. Chang, "Study of vibration and sound characteristics of a copper gong," *J. Chin. Inst. Eng.*, vol. 28, no. 4, pp. 713–719, Jun. 2005, doi: 10.1080/02533839.2005.9671038.

11. N. McLachlan, R. Adams, and C. Burvill, "Tuning natural modes of vibration by prestress in the design of a harmonic gong," *J. Acoust. Soc. Am.*, vol. 131, no. 1, pp. 926–934, Jan. 2012, doi: 10.1121/1.3651255.

12. G. Tsai, B. Wang, Y. Lee, and Z. Chang, "Study of vibration and sound characteristics of a copper gong," *J. Chin. Inst. Eng.*, vol. 28, no. 4, pp. 713–719, Jun. 2005, doi: 10.1080/02533839.2005.9671038.

Laurentius Kevin Hendinata

Laurentius Kevin Hendinata is an Acoustic Engineer at an engineering, climate, and performance consulting firm. He holds an Erasmus Mundus Joint Master's Degree in Waves, Acoustics, Vibrations, Engineering and Sounds (WAVES), jointly awarded by the University of Coimbra, the Polytechnic University of Valencia, and Aix-Marseille University. He received his Bachelor's degree in Engineering Physics from Universitas Gadjah Mada, Indonesia. His professional and research interests include building acoustics, environmental acoustics, noise and vibration control, and numerical modelling for acoustic applications.